10.31653/smf47.2023.249-263

Zhuravlov Yu.I., Kostyuchenko Ye.F., Povar A.I.

National University "Odessa Maritime Academy"

ASSESSMENT OF THE THERMAL AND STRESS-STRAIN STATE OF CYLINDRICAL SURFACES OF SHIP PARTS WITH WEAR-RESISTANT COATINGS

Statement of the problem and its connection with important scientific or practical tasks

Parts of the ship's technical means (STM) in the process of its operation wear out, as a result of which their sizes and shapes change. When parts reach a critical state, failure occurs and repairs are required to restore their performance.

The need for repair may also arise due to a sudden failure caused by jamming of moving joints, jamming of the shutter, breakage of drive parts, equipment, and so on. Parts of STM can be subjected to various types of wear.

The task of the research will be to determine the weakest points of the ship's technical equipment, in particular, the connections of the parts "shaft-sliding bearing" for their quick detection during the incoming inspection. It is also important to compare the criterion dependencies of the gap for two different types of fittings.

The analysis of the situation shows that the prerequisites for the failure of the STM can be divided into four groups [1]:

1 - damage of a factory nature, appearing in case of low-quality initial control of STM at the factory;

2 - damage that occurred during transportation or factory damage that was not detected during incoming inspection;

3 - damage that occurred directly during operation (vibration and erosion-corrosion damage);

4 - damage caused by poor-quality repair of the STM and its components.

Analysis of recent research and publications

There are various types of defects that affect the performance of parts of the ship's technical equipment

Mechanical wear and tear. Mechanical wear occurs as a result of mutual friction of parts (for example, sealing rings of latches, spindle and running nut in their threaded connection, shafts in sliding bearings). As a

result, mechanical wear (wear) depends on the operating forces, the strength and hardness of the metal of the parts, the number of cycles of operation of the STM and the wear resistance of the rubbing surfaces. Oxidative processes occurring in the surface layer of the metal (oxidative wear), processes of microcutting by abrasive particles (abrasive wear), fatigue processes on the metal surface of gear wheels and ball bearings (fatigue wear), processes of metal adhesion, wintering can play a decisive role in mechanical wear, removing roughness.

Erosive wear. Details of ship's technical equipment that perform liquid throttling are subject to erosive wear: plungers and seats of throttling and regulating valves. Wear during erosive wear depends on the throttling mode of the liquid, the duration of its action on the part and the properties of the material of the part. The processes of crevice and impact erosion and cavitation destruction of metal are distinguished. With crevice erosion, the surfaces of the parts are eroded by the action of a jet of wet steam passing at high speed through the gap formed by the saddle and plunger. In impact erosion, the material is destroyed by the impact of water droplets on the surface of the part. In the cavitation mode of movement in the flow of a fast-moving medium and corresponding hydrodynamic conditions, bubbles (voids) are formed as a result of a violation of its integrity. Collapsing, they create local hydraulic shocks, which, acting on the metal surface, destroy it.

Thermal wear. Thermal wear, or thermal aging of metal, is the result of structural transformations that occur in materials during heating. The most characteristic, for example, is the aging of rubber, as a result of which it loses elasticity, becomes brittle. The stuffing box burns out and hardens under the influence of high temperature and pressure.

Chemical wear. Chemical wear occurs as a result of corrosion - the chemical action of working environments on the material of parts of ship's technical equipment. As a result, chemical compounds with low mechanical properties are formed, which are destroyed under the action of force loads or washed out by the working environment. Salts and gaseous substances can be dissolved in condensate and feed water: air oxygen, carbon dioxide, nitrogen, ammonia, hydrogen, etc. However, metal corrosion is caused only by solutions of salts, oxygen and carbon dioxide. Despite desalination and deaeration, a certain amount of substances that cause corrosion of metals remain in the water, as a result of which oxides are formed that settle on the walls of the equipment, including on the surfaces of parts of the ship's technical equipment.

- Corrosion. Corrosion can manifest itself in different ways: general (of the entire metal surface); cracks (cracking of steel); crevice, intercrystalline, pitting (ulcer, point) and others (knife, erosion, selective etching). For STM, the greatest danger is corrosion cracking of steel, which occurs under the simultaneous action of the environment and mechanical stress, including residual stress, for example, created after welding or heat treatment. High-strength steels and alloys are most prone to corrosion cracking: cracks can develop between crystal grains (intercrystalline corrosion) or crossing grains (transcrystalline corrosion).

The listed mechanical, erosive, thermal and chemical wear under known conditions can act simultaneously, which accelerates the failure of parts. Since during the operation of the STM, the wear and tear processes of the parts occur continuously, systematic monitoring of their technical condition is required to detect possible malfunctions.

Setting objectives

The purpose of this study is to determine the weakest parts of the STM, in particular, the combination of "shaft-sliding bearing" parts for their quick detection during incoming inspection.

Key words: ship technical equipment, defects of ship parts, "shaft-sliding bearing" combination, wear of surfaces.

Teaching the main research material

Properties of composite material for ship parts can be considered in two directions. The first are those that depend exclusively on the geometric arrangement of the phases and their corresponding volume fractions, but do not depend on the sizes of the components at all. The second are those that depend on structural factors, such as the periodicity of the arrangement or the sizes of the particles of two or more constituent phases [2-4].

Coefficients of thermal expansion of composites include both elastic constants and coefficients of thermal expansion of individual phases. An important function of reinforcing fillers and fibers in the main material is the reduction and control of thermal expansion [5-8].

The strength of a brittle solid material containing a crack depends on the square root of the crack length. Because very small particles cannot contain long cracks, and because the surface region of most solids behaves differently than the interior (a small fiber or sphere contains proportionally more surface material than a large piece), the tensile strength depends on the size of the part being tested.

The strongest materials are ceramics, consisting of elements from the first rows of the periodic table (B, C, SiC, $A1_2O_3$, etc.). This is because these elements contain the largest possible block of strong covalent bonds directed in three dimensions. Such materials also have a high melting point, low coefficient of thermal expansion, and low density. All of these are highly desirable engineering properties.

Strong fibers, whether rigid or not, also have the great advantage of restraining cracking in so-called brittle matrices (Fig. 1). A crack passing through a brittle material may not penetrate the fibers, but leaves a fiber-lined crack so that the material in which the crack is located is prone to cracking in a large number of places before the fibers themselves fail or pull out.

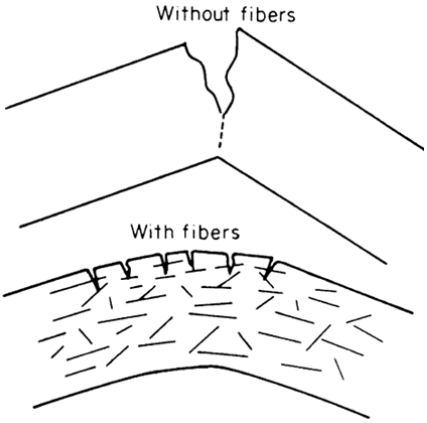

Fig. 1. Demonstration of how fibers prevent cracks in a brittle material from propagating through the fibers into their path

Frictional properties such as wear resistance can, for example, be significantly improved with the help of reinforcing inclusions: the tribological behavior is to some extent determined only by the surface material, it is less important if the reinforcing structure is fibrous or not. Solid ceramic particles added to polymers or metals thus provide very good improvements in wear and abrasion resistance, as well as fibers. An example is aluminum reinforced with SiC particles. This composite is used to make high-performance brake discs, which are strong, light, excellent heat conductors and sufficiently fire-resistant.

Although less effective than with fiber, the viscosity of a brittle matrix can also be improved by adding whiskers, short fibers, or single particles. This can be done using several mechanisms. The reinforcement can be a

much stiffer phase than the matrix, which (provided the crack does not penetrate between particles) prevents crack propagation by forming bridges that bring the crack matrix closer together.

Increases in strength and toughness can be achieved in ceramics undergoing stress-induced transformation [8]. The most impressive is the case of ceramics containing zirconium particles, which represent a tetragonal to monoclinic phase transformation. Using the addition of CeO2 and others, at room temperature you can get a metastable solid tetragonal solution. Under the influence of the applied load, a transformation from martensitic-tetragonal (t) to monoclinic (m) takes place in the vicinity of the crack, which is associated with an increase in volume and shear deformation, which prevent crack propagation and therefore lead to an increase in viscosity. This is an increase ΔK_c^t AKgf, given [9]:

$$\Delta K_c^t = \frac{\eta E e^T V h^{0,5}}{1-\mu},$$

where η is a coefficient that depends on the shape of the transformation zone around the crack, h is its width, E is the effective Young's modulus of the material, V is the volume fraction of transformed particles, e^T is an unbounded deformation transition, μ is Poisson's ratio.

The width of the zone and the volume fraction of the transformed particles depend on the microstructure and especially on the grain size of the material due to the critical stress for the transformation of ac. The larger the grain size, the smaller the ac index, the higher the volume fraction of transformed particles; however, when the grain size becomes larger than the critical size d_e, heating creates conditions for the transformation that occurs during cooling, and most grains are already transformed before crack growth.

When the particle size exceeds the critical size d_e, microcracks appear, which lead to a decrease in the strength of the material [9, 10]. However, if the particle size is smaller than the critical size, microcracks require additional stress that can be provided by the applied load. For effective microcrack reinforcement, the reinforcement must be placed in the technological process zone before the end of the crack. The size of the particles should be as close as possible to the critical size in order to cause significant amplification.

Cracks can be deflected either by stress fields present around the particles or by solid particles of higher resistance. This mechanism leads

to a non-planar crack subject to a mixed failure mode. Regarding discs and rods, the effect of the aspect ratio was investigated. High deflection and, therefore, high stiffness are obtained by rod particles with a high aspect ratio for a volume fraction of about 10-20%.

Cyclic loading contributes to the rate of crack growth and leads to a decrease in the threshold stress. Fatigue behavior can be characterized as the spread of corrosion under load associated with increased degradation [7]. There are several rigid mechanisms (intensification of transformation, bridging of cracks, microcracks).

Residual stress due to thermal mismatch is an important parameter affecting crack resistance. When the coefficient of thermal expansion of the particles is lower than that of the matrix, the composites will most likely resist microcrack development, while, conversely, the crack resistance will be mostly determined by the crack-particle interaction.

A good example of destruction by microcracks is observed in SiC—Al_2O_3 composites: the maximum viscosity occurs as a function of the particle content. The highest strengthening is achieved with the smallest particles, but degradation of strength is observed for large particles, due to the formation of large cracks.

Improvements in creep resistance in other matrices for particle or tube composites are also observed, but generally low. However, excellent resistance to creep is obtained for mulito-zirconium composites and Si_3N_4 composites.

Currently, a new class of structural ceramic materials with effective mechanical properties is being developed. These materials are known as "ceramic nanocomposites", they are obtained by combining a structural ceramic matrix, such as Al_2O_3, ZrO_2 or Si_3N_4, with a nano-sized second phase. Second phases are typically used as "nanoparticles" of 300 nm or less and are added in amounts from 1 vol. % up to 30 vol. % [4]. It was reported that ceramic nanocomposites have both room and high-temperature properties, which significantly exceed the properties of the monolithic matrix in various material systems, which indicates that there is a "structural synergism" of the system between the matrix and the second phase [3-5]. The most widely studied ceramic nanocomposite Al_2O_3-SiC has a promising development.

The processing steps used to obtain nanocomposites have a significant effect on their microstructures and properties. It is well known that the properties of a nanocomposite strongly depend on the dispersion of the second phase [6]. In particular, the uniform dispersion of the second phase

is critical for obtaining the necessary properties in the nanocomposite relative to the monolith. Unfortunately, the spatial distribution of the second phase is very sensitive to the used processing conditions, which indicates that small changes in processing can lead to significant differences in the properties of the nanocomposite.

In nanocomposites with a large volume fraction of the second phase (45 vol%), the matrix grains are equated to a narrow size distribution, and the particles of the second phase are evenly distributed between the matrix grains. An example of this type of microstructure (5 vol.% SiC in Al_2O_3) can be seen in Fig. 2. On the contrary, in samples with a low volume fraction of the second phase, the grain size distribution of the matrix grain can be much wider and in extreme cases there can be anomalous grains.

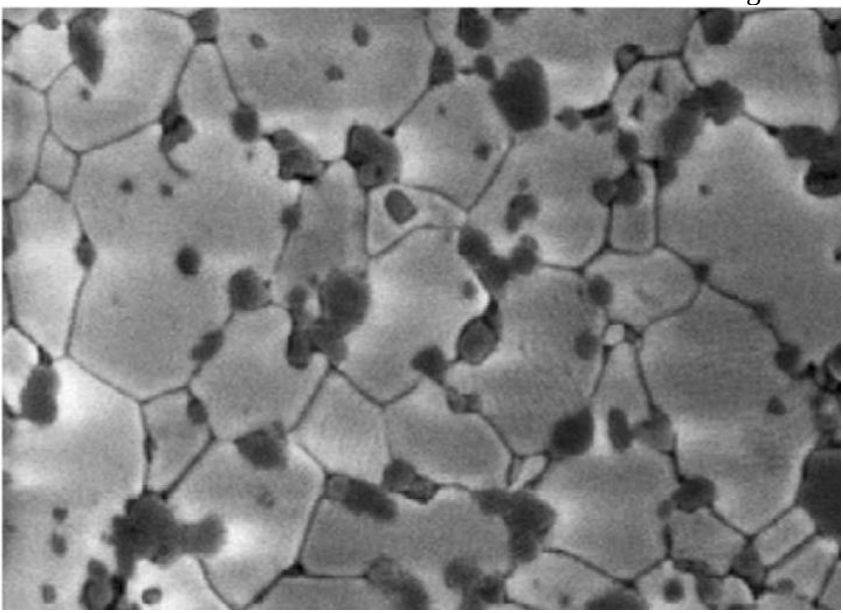

Fig. 2. Scanning electron microscope image of the microstructure of $A1_2O_3$ nanocomposite and 5 vol. % SiC, which shows the presence of both intergranular and intragranular particles

As shown in Fig. 2, the particles of the second phase in the nanocomposite are located either on the grain boundaries (intergranular) or inside the grain (intragranular). In particular, it is believed that intragranular particles are responsible for the excellent properties of the nanocomposite at room temperature, while intergranular particles are responsible for its high-temperature properties. Intergranular particles also

significantly increase the microstructural stability of the nanocomposite. The interaction of particles with grain boundaries strongly inhibits matrix grain growth, which, as a rule, takes place at high temperature. Figure 3 shows SiC particles that inhibit grain growth in the nanocomposite by establishing migrating grain boundaries. The relative proportions of intra- and intergranular particles are strongly related to the grain size of the matrix in the $A1_2O_3$ -SiC system, while the percentage of intergranular particles significantly decreases with grain size. For example, approximately 70% of the particles are expected to be intergranular for a grain size of 1 mm, while 25% of the particles should be intergranular for a grain size of 5 μm [7].

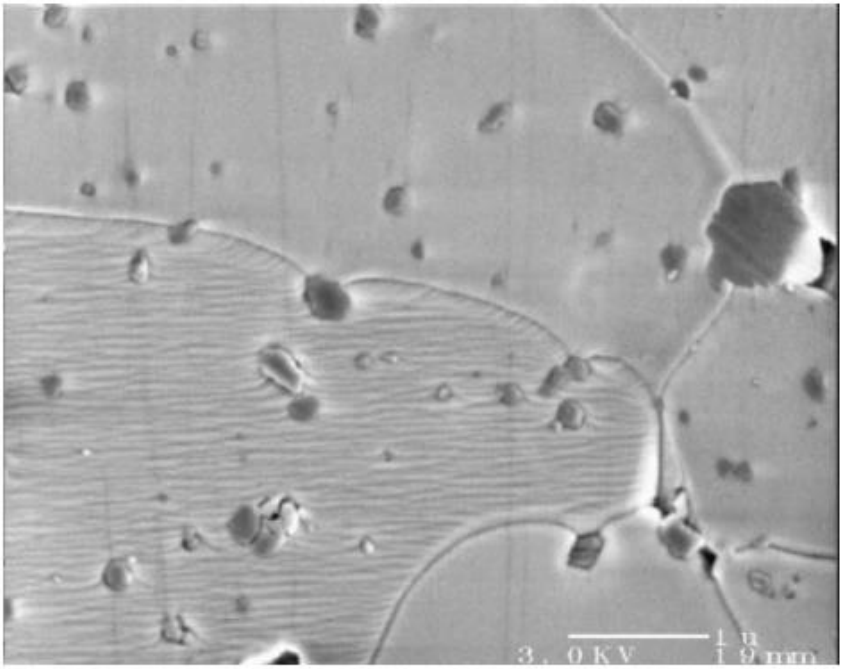

Fig. 3. Image from a scanning electron microscope of SiC particles (5 vol. %) inhibiting grain growth by establishing the migration boundaries of $A1_2O_3$ grains

High-temperature properties of $A1_2O_3$-SiC nanocomposites. The excellent strength and viscosity of the nanocomposite is maintained at room temperature up to 1000 °C [3]. Also, at higher temperatures, the creep resistance of A12O3 is significantly increased due to the presence of 8iC particles [6]. As shown in Fig. 4, the creep rate of $A1_2O_3$ containing 5

vol. % 8iC (150 nm), 2-3 orders of magnitude lower than that of monolithic $A1_2O_3$ at temperatures up to 1300 °C. In addition, the creep duration of the nanocomposite is an order of magnitude longer than that of the monolith. Unfortunately, the deformation index of the nanocomposite is lower than that of $A1_2O_3$, due to the nucleation of intergranular particle cavities. The improved creep resistance of $A1_2O_3$—SiC is explained by a number of mechanisms. These mechanisms include a decrease in the rate of grain diffusion through the boundary of granular particles; inhibition of form placement processes necessary for creep, such as sliding and grain migration; and reducing the internal diffusivity of the A12O3 grain boundary by contamination with silicon cations.

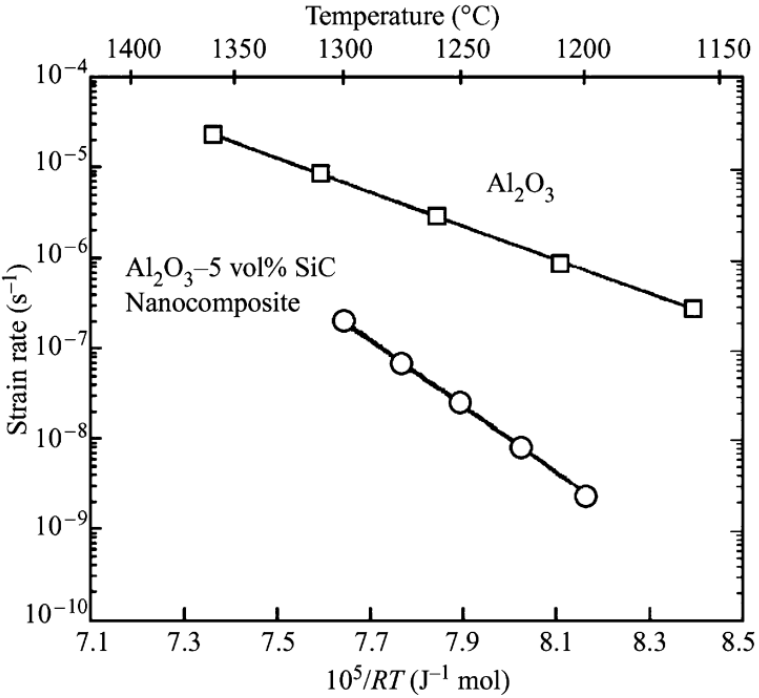

Fig. 4. Diagram of the rate of creep deformation as a function of temperature for monolithic nanocomposites $A1_2O_3$ and $A1_2O_3$ with 5 vol.% SiC [4]

Study of thermomechanical processes in coated products during their processing and operation to determine the conditions for the formation of defects in the coating peeling from the base material and their elimination, taking into account the physical and mechanical condition of the surface layer, technological parameters of the finishing treatment, and hereditary

defects arising in the process application of coatings, show that during translational movement of a cutting tool in a cylinder with out-of-roundness δ (or roughness Ra) in the area (-a; a), zones of partial peeling of the coating are formed on its working surface. Under the influence of working tangential stresses, these areas can reach such values that the coating peels off from the matrix of the cylindrical surface.

Let's find out under which peeling parameters, related to the roughness of the working surface of the cylinder and its geometric error, as well as the physical and mechanical properties of the coating and the material of the cylinder, destruction of its own coating occurs.

The calculation scheme for determining the stress-strain state of the "cylinder-coating" system is given in Fig. 5.

The first step is to consider the equation of thermal conductivity for a two-layer cylinder with symmetrical heating, with free heat exchange with the inner and outer surfaces of the cylinder. The temperature and heat flow in the vicinity of the interface changes continuously.

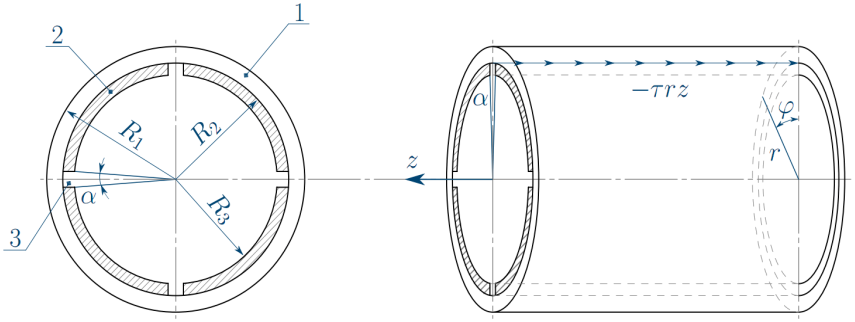

Fig. 5. Calculation scheme for determining the stress-strain state: 1—cylinder body; 2 — coating body; 3 —areas of the absence (exfoliation) of the coating

In other words, we have the following task: to find a continuous function ti(r,τ) in the domain D{ R1≤r≤R3, 0 ≤τ <∞] that satisfies the equation [8-9].

$$\frac{\partial t_i}{\partial \tau} = \alpha_i \left(\frac{\partial^2 t_i}{\partial r^2} + \frac{1}{r} \frac{\partial t_i}{\partial r} \right), \qquad (1)$$

where i =1 for the first region D{ R1≤r≤R3, 0 ≤τ <∞], i =2 for the second region D{R1≤r≤R3, 0 ≤τ <∞]

boundary conditions:

$$\frac{\partial t_1}{\partial r} - h_1\left[t_1 - T_1(\tau)\right] \text{ when } r = R_1,$$

$$\frac{\partial t_2}{\partial r} - h_2\left[t_2 - T_2(\tau)\right] \text{ when } r = R_3; \qquad (2)$$

connection conditions:

$$t_1 = t_2, \quad \lambda_1 \frac{\partial t_1}{\partial r} = \lambda_2 \frac{\partial t_2}{\partial r} \text{ when } r = R_2; \qquad (3)$$

initial condition:

ti{r, 0) = Φi

Here, αi, hi, λi, are the coefficients of thermal conductivity, relative heat transfer, and thermal conductivity, respectively, of the coating (i = 2) and the base material (i = 1).

The functions Φi(r), Ti(τ) satisfy the following conditions:

Ti(τ) is a function differentiated with respect to τ. In addition:

$$\int_0^{\tau}\int_{R_0}^{R_{\Phi i}} \frac{\partial T_i}{\partial \tau}\left[AI_0\left(\gamma_n \frac{r}{\sqrt{\alpha_i}}\right) + BN_0\left(\gamma_n \frac{r}{\sqrt{\alpha_i}}\right)\right]\exp\left[-\gamma_n^2\left(\tau - \bar{\tau}\right)\right]drd\bar{\tau} < \infty \qquad (4)$$

Φi(r) is a continuous function with respect to r, the derivative of which may have a discontinuity

of the first kind at r = R2.

We will look for a solution to problem (1)-(4) in the form:

$$t_i = \left[T_2(\tau) - T_1(\tau)\right]\left(A_i \ln r + B_i\right) + T_i(\tau) + \theta_i(r,\tau). \qquad (5)$$

The solution for θ_i is found by the method of finite integral transforms, the kernels of which $u_{ni}(r)$ are the Bessel equation:

$$u''_{ni} + \frac{1}{r}u'_{ni} + \frac{\gamma_n^2}{\alpha_i}u_{ni} = 0; \qquad (6)$$

with boundary conditions:

$$u'_{ni} - h_1 u_{ni} = 0; \quad npu\ r = R_1; \qquad (7)$$

$$u_{1n} = u_{2n}, \gamma_1 u_{1n} = \gamma_2 u_{2n} \quad npu\ r = R_2;$$

$$u_{2n} + h_2 u_{2n} \quad npu\ r = R_3.$$

The final solution of problems (1)-(4) will be written as follows:

$$t_i(r,\tau)=\psi_i(r,\tau)+\sum_{n=1}^{\infty}\exp\left(-\gamma_n^2\tau\right)\left[\bar{\theta}_n(0)+\int_0^{\tau}\frac{d\bar{\psi}_n(\bar{\tau})}{d\bar{\tau}}\exp\left(-\gamma_n^2\bar{\tau}\right)d\bar{\tau}\right]u_{ni}(r)$$

Here $\psi_i(r,\tau)=\left[T_2(\tau)-T_1(\tau)\right](A_i\ln r+B_i)+T_i(\tau)$.

To determine the stress-strain state of a cylinder with a coating due to the action of a temperature field, consider the following problem. A two-layer unlimited hollow cylinder, on the inner surface of which a temperature field $t_i = t_i(r, \tau)$. acts. The materials of the cylinder and the coating are in contact along the entire surface of the interface and, therefore, the movements on the interface will be continuous. Another condition at the interface is obtained from the condition of continuity of normal stresses σ_r. On the outer surfaces, σg are assumed to be zero. Thus, we have the following problem: to find a continuous function $u_i(r, \tau)$ in the region $D\{R_1 \le r \le R_3, 0 \le \tau < \tau_0]$, which satisfies the equation:

$$\frac{1}{c_i^2}\frac{\partial^2 u_i}{\partial\tau^2}=\frac{\partial^2 u_i}{\partial r^2}+\frac{1}{r}\frac{\partial u_i}{\partial r}-\frac{u_i}{r^2}-m_i\frac{\partial t_i}{\partial r}; \qquad (8)$$

where i = 1 for the first region, i.e. when r changes from R_1 to R_2 and i = 2 for the second region when r changes from R_2 to R_3; $u_i(r,\tau)$ — displacement, C_I — propagation speed of expansion waves in an elastic medium; with boundary conditions:

$$\frac{\partial u_1}{\partial r}+p_1u_1=m_1t_{1,} \qquad when\ r=R_1,$$

$$\frac{\partial u_2}{\partial r}+p_2u_2=m_2t_{2,} \qquad when\ r=R_3 \qquad (9)$$

with connection conditions:

$$u_1=u_2,\frac{\partial u_1}{\partial r}+q_{12}u_1=\frac{\partial u_2}{\partial r}+p_{12}m_1t_1-m_2t_{2,} \quad when\ r=R_2, \qquad (10)$$

with initial conditions:

$$u_i(r,0)=\Phi_i(r),\frac{\partial u_i(r,0)}{\partial\tau}=\psi_i(r), \qquad (11)$$

We will look for a solution to this problem in the form of:

$u_i(r,\tau)=\psi_i(r,\tau)+\theta_i(r,\tau)$

Here

$$\psi_i(r,\tau) = A_i(\tau)r + \frac{B_i(\tau)}{r} + \frac{m_i}{r}\int_{R_i}^{r} t_i(\rho,\tau)\rho\partial\rho$$

quasi-static solution of problem (8)-(11). Ai(τ) and Bi(τ)) are some functions that are chosen so that homogeneous boundary conditions are fulfilled for the function θi(r,τ). The solution obtained for Θi is obtained by the method of finite integral transforms.

The corresponding transform formulas have the form:

$$\vec{\theta}_n = \frac{p_{12}}{c_1^2}\int_{R_1}^{R_2}\theta_1\omega_{1n}rdr + \frac{1}{c_1^2}\int_{R_1}^{R_2}\theta_2\omega_{2n}rdr,$$

$$\theta_i = \sum_{n=1}^{\infty}\vec{\theta}_n\omega_{ni} \quad (R_i \le r \le R_{i+1})$$

Here $\omega_{ni}(r)$ is a solution of Bessel's equations:

$$\omega_{ni}^{n} + \frac{1}{r}\omega_{ni}^{'} + \left(\frac{\gamma_n^2}{c_1^2} - \frac{1}{r^2}\right)\omega_{ni} = 0,$$

with boundary conditions:

$\omega_{1n}^{'} + p_1\omega_{1n} = 0$ *when* $r = R_1$,

$\omega_{1n} = \omega_{2n}, p_{12}\omega_{1n}^{'} + q_{12}\omega_{1n}$ *when* $r = R_2$,

$\omega_{2n} + p_2\omega_{2n} = 0$ *when* $r = R_2$.

to determine Θ_n we have the equation:

$$\frac{d^2\bar{\theta}_n}{d\tau^2} + \gamma_n^2\bar{\theta}_n = -\frac{d^2\bar{\psi}_n}{d\tau^2}, \qquad (12)$$

with initial conditions:

$$\bar{\theta}_n = \bar{\Phi}_n - \bar{\psi}_n, \frac{d\bar{\theta}_n}{d\tau} = \bar{\psi}_n - \frac{d\bar{\psi}_n}{d\tau} \quad npu \quad \tau \qquad (13)$$

The solution of equation (12) with the initial conditions (13) will be written as follows:

$$\bar{\theta}_n = c_{1n}\cos\gamma_n\tau + c_{2n}\sin\gamma_n\tau - \frac{1}{\gamma_n}\int_0^{\tau}\frac{d^2\bar{\psi}_n}{d\tau^2}\sin\left[\gamma_n\left(\tau - \bar{\tau}\right)\right]d\bar{\tau}, \quad (14)$$

where

$$c_{1n} = \bar{\Phi}_n(0) - \bar{\psi}_n(0),\ c_{2n} = \frac{1}{\gamma_n}\left[\bar{\psi}_n(0) - \frac{d\bar{\psi}_n(0)}{d\tau}\right].$$

Conclusions and prospects for further research

1. The mechanism of the formation of defects in the surface layer of ship parts of "shaft-sliding bearing" connections with wear-resistant coatings prone to the formation of cracks is determined.

2. The dependence of the rate of creep deformation as a function of temperature for monolithic nanocomposites Al_2O_3 and Al_2O_3 with 5 vol.% SiC was established.

3. A mathematical model of the thermal and stress-strain state of cylindrical surfaces of ship parts with wear-resistant coatings has been constructed. This approach makes it possible to study processes in heterogeneous environments with variable parameters with the necessary accuracy, which in turn opens up new opportunities for their research.

References

1. Pavlyshyn P. Damage to power valves and their input control. 11 Proceedings of the Odessa Polytechnic University, 2019. - Output. 3(59). - c. 64-67.

2. X-ray Tomography in Material Science / ‚J. Baruchel, G. Peix, ‚J. Y. Buffiere et al. — Hermes Science, 2000. — 1SBX: 9782746201156.— Access mode: https://books.google.com.ua/books?id=RrlRAAAAMAAJ.

3. Bader M. G. Handbook of composite reinforcements // International Materials Reviews. — 2012.— jan. — Vol. 39, no. 3. — P. 123-124.

4. Gay D. Composite Materials: Design and Applications. Third Edition. — 3rd edition. — Boca Raton : CRC Press. 2014. — P. 635. — ISBN: 9780429101038. — Access mode: https : //www. taylorfrancis com/books/9780429101038.

5. Test Methods, Nondestructive Evaluation, and Smart Materials / L. Carlsson, R. L. Crane, K. Ucliino et al. // Comprehensive Composite Materials. — 2000. — Vol. 5.

6. Chawla K. K. Composite Materials: Science and Engineering. Materials Research and Engineering. — New York :Springer, 2013. — ISBN: 9781475739121.—Access mode: https://books.google.com.ua/books7id=87LaBwAAQBAJ

7. Christensen R. M. Mechanics of Composite Materials. Dover Civil and Mechanical Engineering. — Dover Publications, 2012. — ISBN: 978048G136GG0.—Access mode: https://books.google.com.ua/books?id=ean01ydtVc4C.

8. Chou T. W. Microstructural Design of Fiber Composites. Cambridge Solid State Science Series. — Cambridge University Press, 2005.— ISBN: 9780521019651. — Access mode: https://books.google.com.ua/ books7id=pHlER7dPXr4C.

9. Green D. J. Transformation toughening of ceramics. — CRC press, 2019.

10. Pavlyshyn P. Device for electric drives torque diagnostics and its characteristics study // Koroliov A., Kozlov I., Pavlyshyn P., Turmanidze R., Yeputatov Yu. // Lecture notes in mechanical engineering, 2020. - p. 159-165.